

**TITLE: Exome sequencing identifies *MAX* mutations as a cause of hereditary pheochromocytoma**

Iñaki Comino-Méndez<sup>1,2\*</sup>, Francisco J Gracia-Aznárez<sup>2,3\*</sup>, Francesca Schiavi<sup>4\*</sup>, Iñigo Landa<sup>1</sup>, Luis J Leandro-García<sup>1</sup>, Rocío Letón<sup>1</sup>, Emiliano Honrado<sup>5</sup>, Rocío Ramos-Medina<sup>6</sup>, Daniela Caronia<sup>7</sup>, Guillermo Pita<sup>7</sup>, Álvaro Gómez-Graña<sup>1</sup>, Aguirre A de Cubas<sup>1</sup>, Lucía Inglada-Pérez<sup>1,2</sup>, Agnieszka Maliszewska<sup>1</sup>, Elisa Taschin<sup>4</sup>, Sara Bobisse<sup>4</sup>, Giuseppe Pica<sup>8</sup>, Paola Loli<sup>9</sup>, Rafael Hernández-Lavado<sup>10</sup>, José A Díaz<sup>11</sup>, Mercedes Gómez-Morales<sup>12</sup>, Anna González-Neira<sup>7</sup>, Giovanna Roncador<sup>6</sup>, Cristina Rodríguez-Antona<sup>1,2</sup>, Javier Benítez<sup>2,3</sup>, Massimo Mannelli<sup>13</sup>, Giuseppe Opocher<sup>4,14</sup>, Mercedes Robledo<sup>1,2†</sup>, and Alberto Cascón<sup>1,2†</sup>

<sup>1</sup>Hereditary Endocrine Cancer Group, Spanish National Cancer Research Centre (CNIO), Madrid, Spain

<sup>2</sup>Centro de Investigación Biomédica en Red de Enfermedades Raras (CIBERER), Madrid, Spain

<sup>3</sup>Human Genetics Group, Spanish National Cancer Research Centre, Madrid, Spain

<sup>4</sup>Familial Cancer Clinic, Veneto Institute of Oncology, Padova, Italy

<sup>5</sup>Anatomical Pathology Service, Hospital de León, León, Spain

<sup>6</sup>Monoclonal Antibodies Unit, Biotechnology Programme, Spanish National Cancer Research Centre, Madrid, Spain

<sup>7</sup>Human Genotyping Unit-CeGen, Human Cancer Genetics Programme, Spanish National Cancer Centre, Madrid, Spain

<sup>8</sup>Endocrinology and Metabolic Diseases, University of Foggia, Foggia, Italy

<sup>9</sup>Department of Endocrinology, Ospedale Niguarda Ca' Granda, Milan, Italy

<sup>10</sup>Endocrinology Section, Hospital Infanta Cristina, Badajoz, Spain

<sup>11</sup>Department of Endocrinology, Hospital Universitario Clínico San Carlos, Madrid, Spain

<sup>12</sup>Department of Pathology, University Hospital, University of Granada, Spain

<sup>13</sup>Department of Clinical Pathophysiology, University of Florence and Istituto Toscano Tumori, Florence, Italy,

<sup>14</sup>Department of Medical and Surgical Sciences, University of Padova, Padova, Italy

\* These authors contributed equally to this work

†Address correspondence to: Alberto Cascon or Mercedes Robledo

Hereditary Endocrine Cancer Group, Human Cancer Genetics Programme. Centro Nacional de Investigaciones Oncológicas, Melchor Fernández Almagro 3, 28029 Madrid, Spain

Phone: +34-91-224 69 47; Fax: +34-91-224 69 23

e-mail: [acascon@cni.es](mailto:acascon@cni.es); [mrobledo@cni.es](mailto:mrobledo@cni.es)

Hereditary pheochromocytoma (PCC) is often caused by germline mutations affecting one of nine susceptibility genes described so far<sup>1-4</sup>, but there are still familial cases without mutations in these genes. We sequenced the exome of three non-related hereditary PCC patients and found mutations in the MYC associated factor X (*MAX*) gene. Absence of MAX protein in the tumors, and LOH due to uniparental disomy, supported the involvement of *MAX* alterations in the disease. The extended study of a selected series of fifty-nine patients showed five additional *MAX* mutations, and revealed an association with malignant outcome and preferential paternal transmission of *MAX* mutations. The involvement of the MYC/*MAX*/*MXD1* network in the development and progression of neural crest tumors is further supported by the lack of functional MAX in rat PCC (PC12) cells<sup>5</sup> and by the amplification of MYCN in neuroblastoma<sup>6</sup>, and suggests that loss of MAX function is correlated to metastatic potential.

Pheochromocytoma (PCC) is a rare neural crest cell tumor mainly localized within the adrenal medulla, which usually causes secondary hypertension by oversecretion of catecholamines, and which rarely metastasizes. Around 30-40% of patients are familial cases<sup>7,8</sup> exhibiting dominant autosomal inheritance due to germline mutations affecting one of nine susceptibility genes: *RET*, *VHL*, *SDHA*, *SDHB*, *SDHC*, *SDHD*, *SDHAF2*, *NF1*, and *TMEM127*. However, there are still some hereditary cases (<10%)<sup>7,8</sup> not explained by mutations in these genes. Recent gene expression analyses have revealed a common transcriptional profile for tumors carrying germline mutations altering the same gene<sup>9,10</sup>. Moreover, we demonstrated that a subset of tumors from familial PCC patients without germline alterations in the susceptibility genes identified so far exhibited a homogeneous expression profile (GEO accession number: GSE19422)<sup>11</sup>, suggesting that the same as yet unidentified gene could be responsible for these cases.

In the present study, we used Next Generation Sequencing (NGS) to sequence the whole exome of three independent familial PCC patients without any known germline alteration, and whose tumors displayed a common transcriptional profile<sup>11</sup>. Seven HapMap individuals, three males and four females, were also included as quality and filtering controls. Since it is very unlikely that homozygous variants can act as founder mutations, we focused on studying single nucleotide substitutions (SNSs) and small insertions and deletions (INDELs) in heterozygosity. The heterozygous SNSs were selected and consecutively filtered by discarding: i) variants present in the sequenced HapMap controls or in the dbSNP130 database; and ii) variants in intergenic or intronic regions (**Table 1; Supplementary Table 1**). Next, only those variants within coding regions not predicted to produce synonymous aminoacid changes, affecting the same gene in all three samples, and presenting sufficient depth and quality were selected. After that, candidate variants were checked against the last version of dbSNP (dbSNP132) and the 1000 genomes Project data ([www.1000genomes.org/](http://www.1000genomes.org/)). This resulted in only five SNSs, corresponding to two genes

(*MAX* and *ADCY6*), that passed the filtering process. INDEL filtering was performed in a similar manner, but no variant passed the filtering criteria.

After validation by Sanger sequencing, we discarded *ADCY6* as a PCC susceptibility gene because one of the variants (p.Arg1065Gln; **Supplementary Table 1**), did not segregate with the disease in the affected relatives of the family. On the other hand, segregation of *MAX* c.1A>G (p.Met1Val) and c.223C>T (p.Arg75X) variants with the disease was demonstrated in the two families for which DNA from affected relatives was available (**Supplementary Fig. 1**). These variants were not detected in more than 750 population-matched control chromosomes. The three mutations found in *MAX* (**Supplementary Fig. 2a**) were predicted to alter the initiation ATG codon (c.1A>G), introduce a premature stop signal (c.223C>T), and cause exon 4 skipping (c.295+1G>A) (**Supplementary Fig. 2b**). Immunohistochemical analysis of the three PCCs carrying *MAX* mutations demonstrated a lack of full-length *MAX* protein (**Fig. 1**). Next, we analyzed the tumor DNA and found loss of the *MAX* wild type allele in all three cases, indicating loss of heterozygosity (LOH) (**Fig. 2a**). By means of array-CGH analysis, we had previously ruled out the presence of chromosomal losses affecting the *MAX locus* in the same tumors (data not shown). Thus, to decipher the mechanism responsible for the LOH, we carried out a genome-wide single nucleotide polymorphism (SNP) array analysis for one of the tumors and found copy-neutral homozygosity due to uniparental disomy (UPD) affecting almost the entire chromosome 14q (**Fig. 2b**). Multiplex-PCR microsatellite analysis confirmed that the LOH found in the remaining *MAX*-PCCs was also due to UPD (**Fig. 2c**). The paternal origin of the UPD was clear for one of the hereditary cases because of his familial antecedents (**Supplementary Fig. 1a**). To investigate the origin of the UPD in the other two cases, we studied the methylation status of the maternally expressed gene 3 (*MEG3*), an imprinted gene within the disomy region. Only the silenced paternal allele was detected in the tumors of these patients (**Supplementary Fig. 3**), demonstrating that loss of the maternal allele accounted for the LOH in the three cases. Taken

together, these data suggest that *MAX* germline mutations are associated with pheochromocytoma susceptibility, and that *MAX* behaves as a classic tumor suppressor gene.

*MAX* is the most conserved dimerization component of the *MYC/MAX/MXD1* network of basic Helix–Loop–Helix leucine Zipper (bHLHZip) transcription factors that regulate cell proliferation, differentiation, and apoptosis<sup>12</sup>. In this network, *MAX* plays an essential role since it is the common interaction partner for both *MYC* and *MXD1* proteins. While heterodimerization of the *MYC* family of proteins with *MAX* mediates their function as transcription factors, heterodimers of *MAX* with *MXD1* family members (*MXD1*, *MXI1*, *MXD3*, and *MXD4*), *MNT*, and *MGA* antagonize *MYC*-dependent cell transformation by transcriptional repression of the same E-box target DNA sequences<sup>13</sup>. The conservation of the *MAX* sequence is particularly high in the bHLHZip domain, which is involved in protein-protein interactions and DNA binding. In addition, it has been reported that phosphorylation of amino- or carboxy- terminal consensus signals for casein kinase II modulates *MAX* DNA binding properties<sup>14,15</sup>. With respect to PCC, it is well known that PC12 cells, derived from rat adrenal PCC, express a mutant form of *MAX* lacking the carboxyl terminus of the protein which is incapable of repressing transcription from E-box sequences<sup>5,16</sup>. Reintroduction of *MAX* in these cells results in transcriptional repression and reduction in growth rate. These findings suggest that *MAX* disruption leads to an increased cell proliferation, and that *MYC* functions as a transcriptional regulator in spite of the lack of normally functioning *MAX* protein in PCC cells. In addition, the *NRAS/PIK3CA/AKT1/mTOR* axis is essential for the development of PCCs related to oncogenic c-RET-mediated cell transformation<sup>17</sup>, inactivation of the tumor suppressor *NF1*<sup>18</sup>, and mutation of the mTOR regulator *TMEM127*<sup>19</sup>. Since a crosstalk between *NRAS/PIK3CA/AKT1/mTOR* and *MYC/MAX/MXD1* pathways has been reported<sup>20,21</sup>, it is not surprising that alterations in the central regulating protein of the *MYC* network could also lead to PCC development. In agreement with this, it has been reported that *MYC* inhibits *NRAS*-

mediated neuronal differentiation of PC12 cells by blocking c-Jun up-regulation<sup>22</sup>. In addition, amplification and over-expression of MYCN is a genetic hallmark in neuroblastoma<sup>6</sup>, another neural crest cell tumor mainly originated in the adrenal gland. Thus, *MAX* mutations in PCCs could avoid transcriptional repression by MAX of E-box target DNA sequences, leading to oncogenic MYCN deregulation as in neuroblastoma.

We decided to extend the screening of mutations in *MAX* to a selected series of fifty-nine patients without germline alterations in the known susceptibility genes, and who were highly suspected of having hereditary tumors due to the presence of bilateral adrenal PCC, and/or age of onset below 30 years, and/or familial antecedents of the disease (**Supplementary Table 2**). Two additional truncating *MAX* mutations affecting exon 3 (c.97C>T) and 4 (c.185\_186delA), and three missense variants, c.67G>A, c.281T>C, and c.425C>T, located in exons 3, 4 and 5, respectively, were detected (**Table 2**). Immunohistochemical analysis confirmed the lack of full-length MAX in the tumors with truncating variants. The c.67G>A and the c.425C>T variants affect two highly conserved aminoacids, aspartic acid and serine, within two different casein kinase II recognition sites (**Fig. 3**), which suggests that these mutations alter MAX function by modifying its DNA binding abilities. The c.281T>C mutation changed one of the conserved leucines located in the leucine zipper motif of the protein, necessary for MAX protein-protein interactions and oligomerization<sup>23,24</sup>. However, further functional studies are needed to provide direct evidence of the pathogenic character of these three *MAX* missense variants. None of the five new variants were found in controls, and chromosome 14q LOH either due to chromosomal loss or UPD was confirmed in three more tumors (**Table 2**), consistent with a pathogenic role of these *MAX* germline variants. The paternal transmission of the mutation was known in the two hereditary cases, and was confirmed by *MEG3* methylation analysis in other case of which tumor material was available. Acquired segmental UPD is being increasingly recognized as one of the mechanisms of LOH, and therefore constitutes the somatic second hit of Knudson's hypothesis for tumor suppressor genes in a wide variety of neoplasms<sup>25-27</sup>.

Moreover, paternal and maternal chromosome 14 UPD are known to contribute to the development of several malformation syndromes<sup>28</sup>, and interestingly bilateral PCC was recently found in a patient with mosaicism for genome-wide paternal UPD<sup>29</sup>. Taking all these findings into account, it seems that *MAX* is mainly inactivated by this mechanism in the tumors. In addition, the paternal origin of the mutated allele detected in six families suggests a preferentially paternal transmission of the disease (P=0.031). Regarding this, we confirmed both the absence of methylation in various CpG islands of the *MAX* promoter in normal lymphocytes, and the biallelic expression of *MAX* mutations in the mRNA of four patients (data not shown), which ruled out that the expression of this gene is affected by imprinting. This model of inheritance, if confirmed, would constitute the third example of sex-linked transmission in hereditary PCC, besides heritage of mutated *SDHD* and *SDHAF2*<sup>2,30</sup>. The absence of PCC in two children who inherited the mutation from their mother, and in two obliged carriers of a different family further supports this theory (**Supplementary Fig. 1a, c**). The absence of familial antecedents in three of the eight *MAX*-mutated patients with germline mutations is not unusual, and could be due to the suggested preferential paternal transmission. In fact, a substantial proportion of PCC cases with apparently sporadic tumors harbor a germline mutation in one of the susceptibility genes described so far<sup>8</sup>. The appearance of bilateral adrenal PCC in eight of the twelve cases studied (**Table 2**) is in agreement with the association between bilaterality and the presence of germline alterations in PCC patients<sup>8</sup>, and underscores the importance of selecting cases with multiple tumors for the screening of PCC susceptibility genes. In addition, malignant adrenal PCC is a rare condition, with the exception of cases carrying *SDHB* germline mutations. Interestingly, three out of eight probands showed metastases at diagnosis, and another one had familial antecedents of PCC-related malignancy, suggesting the association of *MAX* mutations with PCC aggressiveness.

NGS is steadily attracting interest as one of the most important tools for discovering genes responsible for genetically heterogeneous diseases. Moreover,

exome sequencing represents the best option in this type of agnostic causal variant identification studies over other strategies such as whole genome sequencing. In the present study, NGS allowed us to identify *MAX* as a new PCC tumor suppressor/susceptibility gene. The finding of *MAX* germline mutations in patients with hereditary adrenal tumors agrees with a key role of the MYC/MAX/MXD1 network in the development and progression of neural crest tumors. Moreover, the malignant behavior of *MAX*-related PCCs, similar to neuroblastomas with MYCN amplification, supports the idea that *MAX* loss of function is correlated to metastatic potential. The analysis of a larger series of patients will provide further information about the prevalence of *MAX* mutations in PCC patients, and will clarify the associated *MAX* phenotype which is of fundamental importance for both genetic counseling and genetic testing algorithms.

**Accession codes.** A full listing of the sequencing results have been deposited in ArrayExpress database (accession code: E-MTAB-591).

### **Acknowledgments**

This work was supported in part by the Fondo de Investigaciones Sanitarias (projects PS09/00942 and P1080883 to A.C. and M.R., respectively), Mutua Madrileña (project AP2775/2008 to M.R.), FP7-Grant (ENS@T-CANCER; HEALTH-F2-2010-259735) and Innovation project INTRA-706-2 ISCIII CIBER-ER (Center for Biomedical Research on Rare Diseases). I.C. holds a shuttle CIBER-ER fellowship.

### **Author contributions**

The project was conceived by A.C., M.R., F.S. and G.O. Tumor samples were collected by G. Pica, P.L., R.H-L., J.A.D., M.G.-M. and M.M. Next-generation sequencing analysis and filtering was performed by F.J.G.-A., I.C.-M. and A.C. Additional experiments were performed by I.C.-M., F.J.G.-A., F.S., I.L., L.J.L.-G., R.L., R.R.-M., D.C., A.G.-G., A.A.d.C. L.I.-P., E.T., S.B., A.M., A.G.-N. and G.R. Additional data analysis was performed by A.C., I. C.-M., E.H. and G. Pita. The manuscript was written by A.C., I.C.-M., F.J.G.-A., M.R., C.R.-A. and J.B. All authors approved the final draft.

## Figure legends

**Figure 1.** Detection of MAX by immunohistochemistry with a MAX C-terminus specific antibody. **a**, negative staining of tumor cells in a *MAX*-mutated PCC compared to positive stromal cells (indicated with arrows); **b**, positive staining of a *RET*-mutated PCC; **c**, normal adrenal tissue showing MAX-positive staining.

**Figure 2.** Loss of heterozygosity (LOH) analysis of three *MAX* tumors. **a**, tumor DNA sequence chromatograms of the three *MAX* mutations showing in each case loss of the wild type allele; **b**, SNP array analysis of chromosome 14 performed with tumor DNA from the patient carrying the c.1A>G mutation reveals uniparental disomy (UPD). The lower panel shows the genomic plots of the log R ratio ( $\log_2 R_{\text{patient}}/R_{\text{reference}}$ ) indicating the presence of two alleles, and the upper panel shows the allele frequency parameters along chromosome 14, indicating LOH. Chromosomal locations of *MAX*, *MEG3*, C-14q control, and microsatellites are indicated; **c**, multiplex-PCR microsatellite analysis performed in blood (red) and tumor (blue) DNA from the patient carrying the c.223C>T mutation shows biallelic chromosome 14 amplification, and LOH of the three informative microsatellites due to UPD. C-14q: control amplicon from chromosome 14q; C-1q: control amplicon from chromosome 1q; C-MAX: control amplicon from the *MAX* locus.

**Figure 3.** Schematic representation of *MAX* mutations found in PCC patients. *MAX* transcript 2 (ENST00000358664) contains 5 exons that encode 160 aminoacids, including the bHLHZip domain (denoted with a light grey bar; aminoacids 22 to 102), and the casein kinase II phosphorylation sites (denoted with dark grey bars; numbers indicate the first and the last aminoacid of each site). Truncating and missense mutations are marked with vertical arrows above the gene scheme and below the protein scheme, respectively. At the bottom of the figure the conservation of the three

aminoacids showing missense substitutions in *MAX* (marked with a vertical grey bar) is shown.

**Table 1.** SNSs filtering steps

Sample Nr.	Total number of SNSs	Heterozygous SNSs	SNSs after HapMap control filtering	SNSs after dbSNP130 filtering	SNSs after removing intronic and intergenic variants	SNSs affecting the same gene in the three samples	SNSs in coding regions (not in UTR)	SNSs after removing synonymous, deep<7, and Phred_qual<20	SNSs after removing entries in additional databases†
<b>924</b>	95100	28292	9088	2911	763	41 <sup>§</sup>	17	9	5
<b>3037</b>	92855	26859	7884	3066	789				
<b>3121</b>	89784	26232	8292	3676	743				
<b>Average</b>	92580	27128	8421	3218	765	41	17	9	5
<b>% of SNSs remaining*</b>	100	29.30	9.10	3.48	0.83	0.04	0.02	0.01	0.005

\* , percentage of SNSs after each filtering step; †, 1000genomes and dbSNP132; §, a complete list of these variants is shown in Supplementary Table 1.

**Table 2.** Clinical features of patients with *MAX* mutations

Family	ID	Sex	Age at onset	Familial antecedents	Tumor	Malignant	Mutation cDNA*	Mutation protein*	Tumor 2 <sup>nd</sup> hit	p <i>MEG3</i>
<b>a</b>	<b>3121</b>	M	29	yes <sup>P</sup>	bPCC	no	c.223C>T	p.Arg75X	UPD	yes
a	3119	M	35	-	bPCC	no	c.223C>T	p.Arg75X	na	na
a	1090	F	34	-	bPCC	no	c.223C>T	p.Arg75X	na	na
a	3122	F	28	-	bPCC	no	c.223C>T	p.Arg75X	na	na
<b>b</b>	<b>3037</b>	M	32	yes <sup>U</sup>	bPCC	yes	c.295+1G>A	p.?	UPD	yes
<b>c</b>	<b>924<sup>†</sup></b>	F	46	yes <sup>U</sup>	bPCC	yes	c.1A>G	p.Met1?	UPD	yes
c	922	M	29	-	PCC	no	c.1A>G	p.Met1?	na	na
d	190	M	17, 20	no	bPCC	no	c.97C>T	p.Arg33X	14q loss	yes
e	1016	F	47	yes <sup>P</sup>	bPCC	no	c.185_186del A	p.Gln62AsnfsX 23	14q loss	yes
f	368	F	26	no	PCC	yes	c.67G>A	p.Asp23Asn	na	na
g	1075	F	22	no	PCC	no	c.425C>T	p.Ser142Leu	na	na
h	F31S	F	41	yes <sup>P</sup>	PCC	no	c.281T>C	p.Leu94Pro	UPD	yes

<sup>†</sup>, deceased; bPCC, bilateral adrenal pheochromocytoma; the three cases sequenced are shown in bold; <sup>P</sup>, paternal familial antecedents; <sup>U</sup>, unknown; UPD, uniparental disomy; na, not available; p*MEG3*, exclusive paternal *MEG3* allele detection; \*, All cDNA and protein nomenclature is based on reference sequence ENST00000358664

## **Methods**

**Patients and controls.** Included patients were clinically diagnosed with functioning or non-functioning adrenal PCC in Spanish and Italian public hospitals. All tested negative for mutations in the seven major PCC susceptibility genes: *VHL*, *RET*, *SDHB*, *SDHC*, *SDHD*, *SDHAF2*, and *TMEM127*. Genomic DNA was extracted from the patients' blood following a standard method<sup>31</sup>. Tumor DNA from frozen and paraffin-embedded tissues was obtained using the DNeasy kit (Qiagen Inc., Valencia, CA, USA), following the manufacturer's instructions. Informed consent was obtained from all patients. DNAs from at least 375 unrelated, unaffected individuals were analyzed as controls. HapMap DNAs used as quality and filtering controls for NGS were extracted from the cell lines of seven individuals of European-American ancestry (NA11881, NA12144, NA12750, NA12761, NA12763, NA12813, NA12892) originally sourced from Coriell Cell Repositories.

**Whole exome enrichment and NGS.** DNA samples from patients and controls were enriched for exomic regions according to Agilent's SureSelect Human All Exon Kit protocol (Agilent Technologies, Palo Alto, CA, USA). Resulting DNA libraries were sequenced using 78 base pairs, paired-end technology on an Illumina Genome Analyzer II (Illumina, San Diego, CA, USA), following the manufacturer's protocol. Two sequencing lanes per sample were used in order to obtain sufficient sequencing depth for the final variant analysis. Real-time image analysis and base calling was performed using Illumina's Real Time Analysis software version 1.6 using standard parameters.

**NGS data Analysis.** Unaligned data from each of the four sequence files generated per individual (two files per sequencing lane, one for each of the pair-ends) were merged into two files, one containing the information for the first sequencing pair for both lanes and the other containing the corresponding information for the other pair. Both files were then filtered coordinately to remove low quality reads (containing 6 or more undefined bases), homopolymers, and dinucleotide repetitions using an in-house

developed Perl script (Quality-Control-1). Filtered files were aligned against the whole human genome (hg18 assembly) using Novoalign version 2.06.09 ([www.novocraft.com](http://www.novocraft.com)). Standard alignment settings were used except for the gap extension penalty (set to 5) and the option of reporting up to 3 alignment locations for those reads matching more than one region on the genome. Aligned SAM files were sorted by chromosome and coordinate and then analyzed with the Perl script Read\_selection, in order to select on-target reads with sufficient quality for subsequent analysis. Samtools version 0.1.8<sup>32</sup> was used to remove PCR duplicates (rmdup option), and for variant calling (pileup option). SNS and INDEL data was extracted from pileup files using a Perl script (Pileup4annotation), which also calculated two scores: Deep Score and Quality-Score (**Supplementary Table 1**). These scores represent a ratio between the read depth (deep) or the Phred-scaled quality score for the variant allele (Xv) and the reference allele (Xr):

$$\text{Deep Score (or Quality Score)} = \left( \frac{X_v}{X_r} \right) \times 100$$

**Variant selection.** SNS and INDEL data were analyzed separately. Using a series of newly-developed Perl scripts, they were first confronted against two sets of variants (SNSs and INDELS, respectively) obtained from the seven HapMap controls using specific thresholds (see above) (**Table 1**). This comparison was performed with Perl scripts (Comp\_against\_controls-SNSs, Comp\_against\_controls-INDELS). Next, both variant types were filtered against the information in dbSNP130, and annotated using the Ensembl database in Annovar<sup>33</sup>. Variants in intergenic or intronic regions were subsequently discarded and high quality variants (Deep>7 and Phred Quality>20) affecting the same gene in all three samples and not producing synonymous aminoacid changes in the resulting protein were selected.

**MAX Sanger sequencing.** Primers spanning the five exons of the major MAX transcript (ENST00000358664) were used to amplify germline DNA from the selected

PCC patients. The purified products were subsequently sequenced using the automatic sequencer ABI 3730xl (Applied Biosystems, Perkin Elmer, USA). Primer sequences and PCR conditions are available upon request.

**RT-PCR.** Total RNA was isolated from frozen tumor tissue carrying the mutation c.295+1G>A using the TriReagent kit (MRC, Cincinnati, OH, USA), following the manufacturers' instructions. First strand cDNA was synthesized from 2 µg of total RNA by oligo(dT)14 primer reverse transcription with Superscript II Reverse Transcriptase (Invitrogen, CA, USA) following the manufacturer's instructions. A PCR was then performed to generate a fragment spanning exons 1-5 of MAX transcript 2 (ENST00000358664) using the primers included in **Supplementary Table 3**. The PCR products were analyzed by electrophoresis on a 2% agarose gel. cDNA from peripheral blood lymphocytes of a healthy volunteer was used as control.

**Loss of heterozygosity (LOH) and uniparental disomy (UPD) analyses.** LOH analysis of the *MAX* locus was performed on seven tumors for which blood and tumor DNA were available. We first performed direct sequencing of tumor DNA using the same PCR conditions as applied for germline DNA. To investigate the origin of the LOH found in the tumors we performed High Density Single Nucleotide Polymorphism-array (SNP-array) analysis in one of the tumors. A genome-wide scan of 616,795 markers was conducted on 250 ng of tumor DNA, using the Illumina Human610-Quad BeadChip according to the manufacturer's specifications. Image data was analyzed using the Chromosome Viewer tool contained in GenomeStudio 2010.2 (Illumina). The metric used was the log R ratio which is the log ratio of the observed normalized R value for a SNP divided by the expected normalized R value<sup>34</sup>. In addition, an allele frequency analysis was applied for all SNPs. UPD or chromosomal loss was assessed in the other *MAX*-tumors by microsatellite analysis. Three polymorphic markers spanning chromosome 14 from the *MAX* locus to the telomere were selected (Supplementary Table 3) and analyzed by multiplex amplification. We first designed

and labeled (5' 6-FAM) a pair of primers for each marker. We used labeled control fragments from *MAX* and from chromosomes 1q and 14q as internal controls. We amplified genomic and tumor DNA separately by means of a multiplex PCR kit (Qiagen, GmbH, Hilden, Germany), as previously described<sup>35</sup>. Purified PCR amplification products were used for fragment analysis on an ABI PRISM™ 310 capillary sequencer (Applied Biosystems, Foster City, CA, USA), and analyzed using Peak Scanner™ Software v1.0 (Applied Biosystems). Normalization was performed by overlapping each patient sample with the corresponding tumor sample, determining the peak surface of all fragments and calculating the normal peak fractions. A second multiplex-PCR that included control peaks from three different regions (chromosomes 5, 12, and 15), as well as one *MAX* amplicon and two 14q fragments, was performed to determine the loss of chromosome 14q. Finally, we genotyped various subtelomeric SNPs (Supplementary Table 3) both in blood and tumor DNA to assess the extension of the LOH.

**Methylation of Maternally Expressed Gene 3 (*MEG3*).** To demonstrate the paternal origin of the mutated allele, we analyzed the methylation status of the *MEG3* promoter in six cases for which tissue was available by conventional methylation-specific PCR, using previously described primers and conditions<sup>36</sup>. Bisulphite treatment of tumor DNA was performed using the EZ DNA methylation kit (Zymo Research) according to the manufacturer's instructions. DNA from normal lymphocytes and from a RET-PCC were used as controls. PCR products were visualized by ethidium bromide staining after 2.5% agarose gel electrophoresis. A 160 bp PCR product represented the methylated state, while a 120 bp PCR product corresponded to the unmethylated maternal allele of *MEG3*. Statistical evidence for paternally transmission was assessed by a two-tailed binomial test using R version 2.9.0 (<http://www.r-project.org>).

***MAX* protein analyses.** Prior to demonstrating the absence of full-length *MAX* in tumors carrying *MAX* truncating mutations, we evaluated the specificity of the sc-197

antibody (Santa Cruz Biotechnology, CA, USA) by western blot in HeLa, Jurkat, and PC12 cells (**Supplementary Fig. 4**). This is a commercial polyclonal antibody raised against the C-terminus of the human MAX protein that specifically recognizes translated MAX transcripts 1 (ENST00000358402) and 2 (ENST00000358664). Proteins were separated by 4-12% SDS-PAGE and transferred to a polyvinylidene fluoride membrane, as previously described<sup>37</sup>. The membrane was blocked and then incubated with a 1:200 dilution of the antibody following the manufacturer's instructions. Equal protein loading was assessed using a 1:12,000 dilution of anti-beta actin antibody (A5441, Sigma, MO, USA). Immunohistochemical staining was performed using 3 µm formalin-fixed paraffin embedded tumor sections from the five PCCs carrying truncating MAX mutations. Two normal adrenal sections and ten tumors carrying mutations in other PCC susceptibility genes (*RET*, *NF1*, *SDHB*, *SDHD*, and *TMEM127*) were used as controls. After drying the sections in a 60°C oven overnight, they were placed in a Bond MAX Automated Immunohistochemistry Vision Biosystem (Leica Microsystems GmbH, Wetzlar, Germany) according to the following protocol. First, tissues were deparaffinized and pre-treated with Epitope Retrieval Solution 2 (EDTA-buffer pH8.8) at 98°C for 20 min. After several washing steps, peroxidase blocking was carried out for 10 min using the Bond Polymer Refine Detection Kit DC9800 (Leica Microsystems GmbH). Tissues were again washed and then incubated with sc-197 MAX primary antibody (1:1600) for 30 min. Subsequently, tissues were incubated with polymer for 15 min and developed with DAB-Chromogen for 10 min. Only cases showing nuclear staining of stromal cells were considered as evaluable.

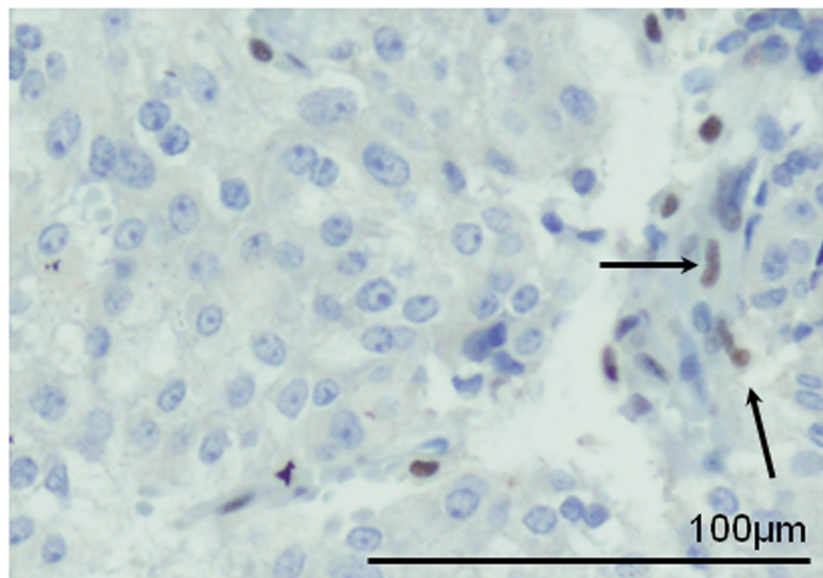
## References

1. Neumann, H.P. et al. Germ-line mutations in nonsyndromic pheochromocytoma. *N Engl J Med* **346**, 1459-66 (2002).
2. Hao, H.X. et al. SDH5, a gene required for flavination of succinate dehydrogenase, is mutated in paraganglioma. *Science* **325**, 1139-42 (2009).
3. Yao, L. et al. Spectrum and prevalence of FP/TMEM127 gene mutations in pheochromocytomas and paragangliomas. *JAMA* **304**, 2611-9 (2010).
4. Burnichon, N. et al. SDHA is a tumor suppressor gene causing paraganglioma. *Hum Mol Genet* **19**, 3011-20 (2010).
5. Hopewell, R. & Ziff, E.B. The nerve growth factor-responsive PC12 cell line does not express the Myc dimerization partner Max. *Mol Cell Biol* **15**, 3470-8 (1995).
6. Kohl, N.E. et al. Transposition and amplification of oncogene-related sequences in human neuroblastomas. *Cell* **35**, 359-67 (1983).
7. Mannelli, M. et al. Clinically guided genetic screening in a large cohort of italian patients with pheochromocytomas and/or functional or nonfunctional paragangliomas. *J Clin Endocrinol Metab* **94**, 1541-7 (2009).
8. Cascon, A. et al. Genetics of pheochromocytoma and paraganglioma in Spanish patients. *J Clin Endocrinol Metab* **94**, 1701-5 (2009).
9. Favier, J. et al. The Warburg effect is genetically determined in inherited pheochromocytomas. *PLoS One* **4**, e7094 (2009).
10. Dahia, P.L. et al. A HIF1alpha regulatory loop links hypoxia and mitochondrial signals in pheochromocytomas. *PLoS Genet* **1**, 72-80 (2005).
11. Lopez-Jimenez, E. et al. Research resource: Transcriptional profiling reveals different pseudohypoxic signatures in SDHB and VHL-related pheochromocytomas. *Mol Endocrinol* **24**, 2382-91 (2010).
12. Atchley, W.R. & Fitch, W.M. Myc and Max: molecular evolution of a family of proto-oncogene products and their dimerization partner. *Proc Natl Acad Sci U S A* **92**, 10217-21 (1995).
13. Grandori, C., Cowley, S.M., James, L.P. & Eisenman, R.N. The Myc/Max/Mad network and the transcriptional control of cell behavior. *Annu Rev Cell Dev Biol* **16**, 653-99 (2000).
14. Bousset, K., Henriksson, M., Luscher-Firzlaff, J.M., Litchfield, D.W. & Luscher, B. Identification of casein kinase II phosphorylation sites in Max: effects on DNA-binding kinetics of Max homo- and Myc/Max heterodimers. *Oncogene* **8**, 3211-20 (1993).
15. Prendergast, G.C., Hopewell, R., Gorham, B.J. & Ziff, E.B. Biphasic effect of Max on Myc cotransformation activity and dependence on amino- and carboxy-terminal Max functions. *Genes Dev* **6**, 2429-39 (1992).
16. Ribon, V., Leff, T. & Saltiel, A.R. c-Myc does not require max for transcriptional activity in PC-12 cells. *Mol Cell Neurosci* **5**, 277-82 (1994).
17. Segouffin-Cariou, C. & Billaud, M. Transforming ability of MEN2A-RET requires activation of the phosphatidylinositol 3-kinase/AKT signaling pathway. *J Biol Chem* **275**, 3568-76 (2000).
18. Johannessen, C.M. et al. The NF1 tumor suppressor critically regulates TSC2 and mTOR. *Proc Natl Acad Sci U S A* **102**, 8573-8 (2005).
19. Qin, Y. et al. Germline mutations in TMEM127 confer susceptibility to pheochromocytoma. *Nat Genet* **42**, 229-33 (2010).
20. Zhu, J., Blenis, J. & Yuan, J. Activation of PI3K/Akt and MAPK pathways regulates Myc-mediated transcription by phosphorylating and promoting the degradation of Mad1. *Proc Natl Acad Sci U S A* **105**, 6584-9 (2008).

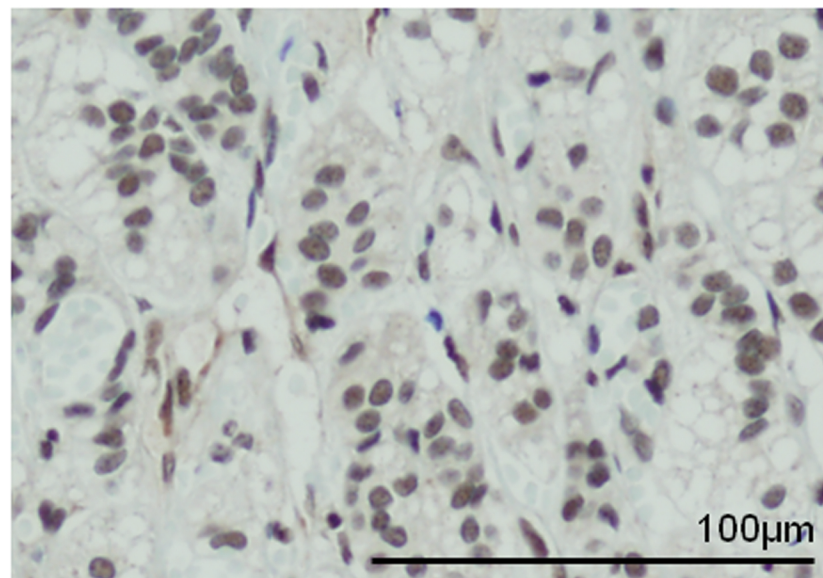
21. Jimenez, R.H. et al. Regulation of gene expression in hepatic cells by the mammalian Target of Rapamycin (mTOR). *PLoS One* **5**, e9084.
22. Vaque, J.P. et al. c-Myc inhibits Ras-mediated differentiation of pheochromocytoma cells by blocking c-Jun up-regulation. *Mol Cancer Res* **6**, 325-39 (2008).
23. Nair, S.K. & Burley, S.K. X-ray structures of Myc-Max and Mad-Max recognizing DNA. Molecular bases of regulation by proto-oncogenic transcription factors. *Cell* **112**, 193-205 (2003).
24. Dang, C.V., McGuire, M., Buckmire, M. & Lee, W.M. Involvement of the 'leucine zipper' region in the oligomerization and transforming activity of human c-myc protein. *Nature* **337**, 664-6 (1989).
25. Teh, M.T. et al. Genomewide single nucleotide polymorphism microarray mapping in basal cell carcinomas unveils uniparental disomy as a key somatic event. *Cancer Res* **65**, 8597-603 (2005).
26. Murthy, S.K., DiFrancesco, L.M., Ogilvie, R.T. & Demetrick, D.J. Loss of heterozygosity associated with uniparental disomy in breast carcinoma. *Mod Pathol* **15**, 1241-50 (2002).
27. Tiu, R.V. et al. New lesions detected by single nucleotide polymorphism array-based chromosomal analysis have important clinical impact in acute myeloid leukemia. *J Clin Oncol* **27**, 5219-26 (2009).
28. Kurosawa, K. et al. Paternal UPD14 is responsible for a distinctive malformation complex. *Am J Med Genet* **110**, 268-72 (2002).
29. Wilson, M. et al. The clinical phenotype of mosaicism for genome-wide paternal uniparental disomy: two new reports. *Am J Med Genet A* **146A**, 137-48 (2008).
30. Baysal, B.E. et al. Mutations in SDHD, a mitochondrial complex II gene, in hereditary paraganglioma. *Science* **287**, 848-51 (2000).
31. Sambrook, J., Maniatis, T. & Fritsch, E.F. *Molecular cloning : a laboratory manual*, 3 v. (Cold Spring Harbor Laboratory, Cold Spring Harbor, N.Y., 1989).
32. Li, H. et al. The Sequence Alignment/Map format and SAMtools. *Bioinformatics* **25**, 2078-9 (2009).
33. Wang, K., Li, M. & Hakonarson, H. ANNOVAR: functional annotation of genetic variants from high-throughput sequencing data. *Nucleic Acids Res* **38**, e164.
34. Simon-Sanchez, J. et al. Genome-wide SNP assay reveals structural genomic variation, extended homozygosity and cell-line induced alterations in normal individuals. *Hum Mol Genet* **16**, 1-14 (2007).
35. Cascon, A. et al. Gross SDHB deletions in patients with paraganglioma detected by multiplex PCR: a possible hot spot? *Genes Chromosomes Cancer* **45**, 213-9 (2006).
36. Astuti, D. et al. Epigenetic alteration at the DLK1-GTL2 imprinted domain in human neoplasia: analysis of neuroblastoma, pheochromocytoma and Wilms' tumour. *Br J Cancer* **92**, 1574-80 (2005).
37. Landa, I. et al. Allelic variant at -79 (C>T) in CDKN1B (p27Kip1) confers an increased risk of thyroid cancer and alters mRNA levels. *Endocr Relat Cancer* **17**, 317-28 (2010).

Figure 1

**a**



**c**



**b**

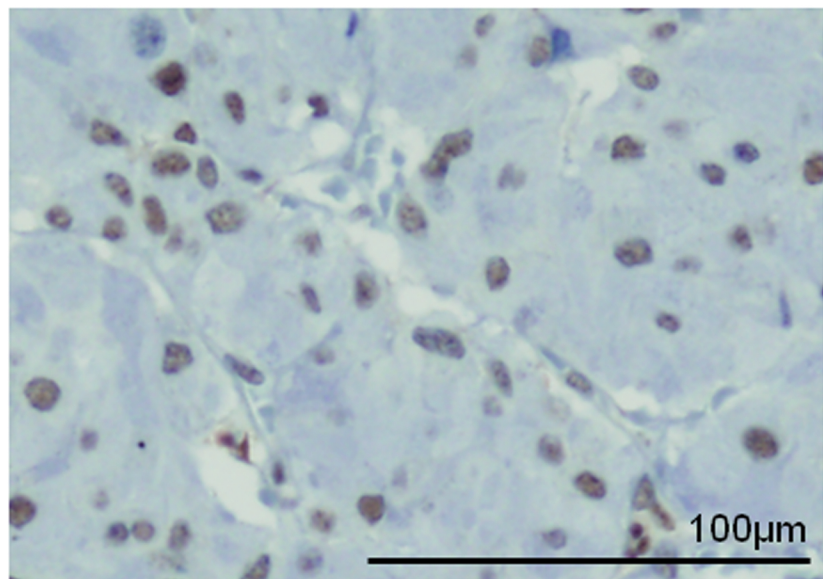
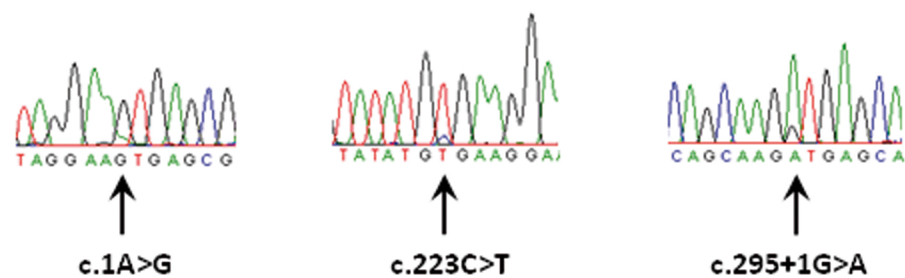
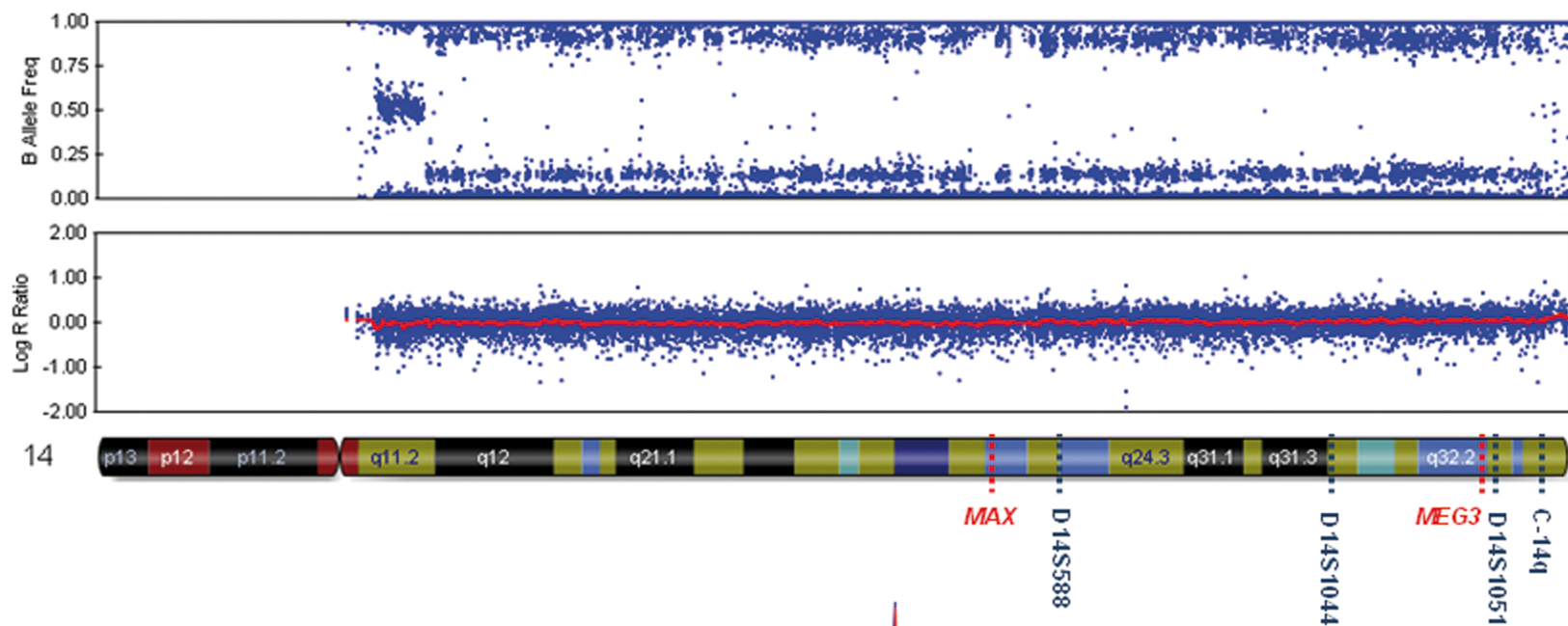


Figure 2

**a**



**b**



**c**

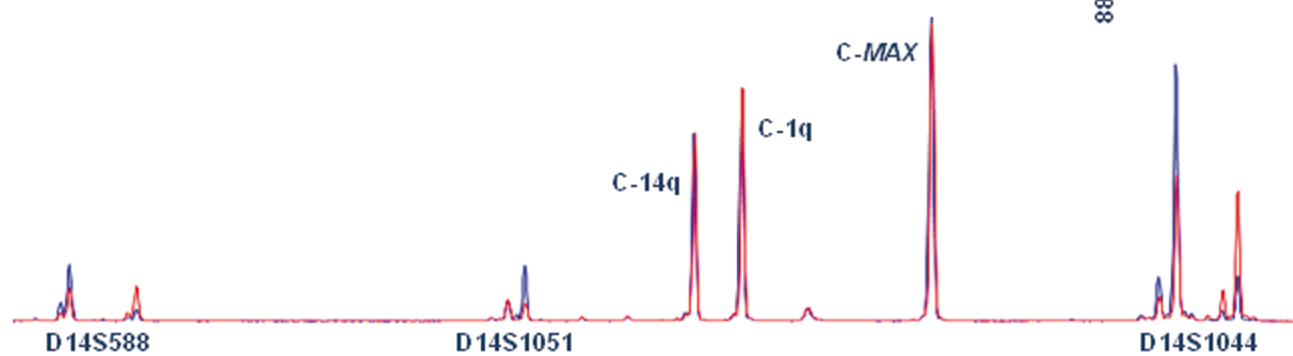


Figure 3

